

The Canada-France Redshift Survey VII: Optical counterparts of microJansky radiosources

F. Hammer,^{1*} David Crampton,^{2*} Simon J. Lilly,^{3*} O. Le Fèvre,^{1*} T. Kenet³

¹ *DAEC, Observatoire de Meudon, Meudon, 92195, France*

² *Dominion Astrophysical Observatory, National Research Council of Canada, Victoria, V8X 4M6 Canada*

³ *Department of Astronomy, University of Toronto, Toronto, M5S 1A7 Canada*

Accepted . Received 1994 December

ABSTRACT

Deep imaging and spectroscopy have been carried out for optical counterparts of a complete sample of $S > 16 \mu\text{Jy}$ radiosources during the course of the Canada-France Redshift Survey (CFRS). All 36 sources but two have been optically identified, and spectra have been obtained for 23 of them. The objects brighter than $I_{AB} < 22.5$ for which we have spectra reveal three populations dominating the μJy radio counts: $z > 0.7$ early-type galaxies with radio emission powered by an AGN, intermediate redshift post-starburst galaxies, and lower redshift blue emission-line objects. From their radio and optical properties, it is argued that the 11 objects fainter than $I_{AB} > 22.5$ are mostly at $z > 1$, and one half of them are probably early-type galaxies. We conclude that ~ 40 per cent of the μJy sources are likely to be at $z > 1$.

Between one third and one half of the luminous ellipticals in this field beyond $z = 0.7$ show moderately powerful radio emission ($P \sim 5 \cdot 10^{23} \text{ W Hz}^{-1}$) which is at least 10 times more powerful than seen in local samples, and probably reflects evolution of the activity in their nuclei. Only one classical starburst galaxy is identified in the sample; the rest of the blue emission-line objects show optical and radio activity more typical of low power AGNs than starbursts. The number of post-starbursts at μJy levels is considerably higher than the surface density of mJy starburst galaxies, suggesting the latter are the parent population of the former. While starburst galaxies are considered to be major contributors to the mJy radiosources counts, the majority of the μJy radio sources appear to be related to AGN activity rather than to normal star formation.

Key words: galaxies:active – galaxies:starburst – radio continuum: galaxies

1 INTRODUCTION

Deep 1.4GHz counts show an upturn below a few milliJanskys (mJy), corresponding to a rapid increase in the number of faint sources (Windhorst, 1984; Condon and Mitchell, 1984; Oort and Windhorst, 1985), with a decreasing fraction of sources which can be ascribed to elliptical galaxies and QSOs. Several scenarios have been developed to interpret this numerous new population, invoking either a non-evolving population of low redshift galaxies at very low radio power (Wall et al. 1986) or strong evolution of normal spirals at $z > 0.1$ (Condon 1989). The latter scenario is sup-

ported by the spectroscopic work of Benn et al. (1993), who identified the brightest optical counterparts of sub-mJy radiosources as $z \sim 0.2$ blue galaxies which they interpreted as starburst galaxies. However, there is little information about the true redshift distribution of the sub-mJy population because only a small fraction of them have been identified and have measured redshifts (Rowan-Robinson et al. 1993). Towards the μJy levels ($\sim 16 \mu\text{Jy}$ at 4.86GHz), the projected number density of radiosources reaches the number density of $B = 21.5$ field galaxies, while the fraction of flat spectrum radiosources is increasing continuously (Fomalont et al. 1991, hereafter FWKK). Because of this high surface density, the understanding of μJy radiosources may provide new and interesting constraints on the evolution of field galaxies.

During the preliminary deep imaging phase of our large spectroscopic survey of faint field galaxies (CFRS), one of our fields was chosen to coincide with the FWKK ra-

* Visiting Astronomer, Canada-France-Hawaii Telescope, which is operated by the National Research Council of Canada, the Centre de Recherche Scientifique of France, and the University of Hawaii

diosource field (see Tresse et al. 1993). This field – as with other CFRS fields – is at high Galactic latitude ($b^{II} \sim 60^\circ$). We present here the results of the observations of 36 objects which represent a complete sample of μJy radiosources. Although we were only able to acquire spectra for objects with $I_{AB} \leq 22.5$, the colours and radio spectral indices of the fainter objects enable us to investigate the properties of the entire radio sample.

2 OPTICAL IDENTIFICATION, PHOTOMETRY, AND SPECTROSCOPY

2.1 Photometry and optical morphology

The field at 1415+52 is one of the five $10' \times 10'$ fields selected for the CFRS survey of $I_{AB} \leq 22.5$ galaxies. BVI photometry was carried out at CFHT with FOCAM, to a depth well beyond the spectroscopic limits to ensure that there was no bias against low surface brightness objects. The image quality was generally excellent, ranging from $\text{FWHM} = 0''.7 - 0''.9$. K' band photometry was also obtained at CFHT with RedEye on roughly one-third of the spectroscopic objects. Details of the data reduction and photometric limits are presented in CFRS I: Lilly et al. 1994. Throughout this paper the AB system is used, where $V_{AB} = V$, $I_{AB} = I + 0.48$, $K_{AB} = K + 1.78$.

The depth and quality of our images also allows us to examine the morphology of all of the optical counterparts. The CCD pixel sizes of the B, V and I images are $0''.207$ and the FWHM of point sources are typically 2.4 pixels after deconvolution. Sources were systematically deconvolved in the I frame, and very often in the V frame, using the MEM tool of the IRAF STSDAS package and a relatively bright star selected as close as possible to the source.

2.2 Astrometry

In order to derive very accurate astrometric positions for the objects on our FOCAM images, accurate positions of several secondary standard stars in the field were utilized. To accomplish this, accurate positions of 18 HST Guide Star Catalogue (GSC) stars were measured with a two-coordinate measuring machine on POSS E plates in an area which included the CCD field, plus the positions of 16 stars which were unsaturated on the CCD. An astrometric plate solution for the GSC star positions was then used to relate pixel positions of the 16 stars on the CCD image to their astrometric positions, with a formal RMS error $0''.46$, and to develop a similarly precise mapping of pixel positions to celestial coordinates for all objects in the field. As will become apparent below, the resulting positions for the optical counterparts are in excellent agreement with the radio source positions.

FWKK list 62 sources in their complete ($S > 16 \mu\text{Jy}$) sample; 40 of these lie in our survey field. One source (15V56) has to be excluded from our subsample since it lies in the outskirts of a bright nearby galaxy, preventing optical identification to any reasonable depth (as noted below, others were subsequently deleted for other reasons, reducing

the number to 36). We have been very successful in identifying virtually all of the remaining sources with optical counterparts on our images. Comparison of the optical and radio positions of 19 sources which are isolated (no confusing adjacent sources), and which are obvious, certain identifications, demonstrates that the optical and radio reference frames are in perfect agreement (to better than $0''.15$). The random error, as indicated by the RMS residual in the optical and radio positions for these sources, is $0''.54$.

2.3 Spectroscopy

Spectroscopic observations of 11 of the counterparts were obtained with the CFHT MOS/SIS multi-object spectrographs as part of the CFRS survey, and subsequently an additional 12 were specifically targeted in order to achieve reasonable completeness. Including a few objects observed by Tresse et al. (1993), spectra of 22 of the 25 counterparts in the double-limited sample ($S > 16 \mu\text{Jy}$ and $I_{AB} \leq 22.5$) were obtained. The spectral resolution was 40\AA , and integration times ranged from 7^h to 9^h (7 to 9 times one hour integration). The methodology adopted for data reduction, redshift identification and reliability is discussed in detail in CFRS II: Le Fèvre et al. (1995), and data for other objects in this field are given in CFRS III: Lilly et al. (1995).

2.4 Identifications

A summary of the results of our identifications, photometry and spectroscopy for all 39 sources is given in Table 1. FWKK's source number and radio (5 GHz) flux are listed in the first two columns, followed by the number of the optical counterpart in the CFRS catalogue. The isophotal I_{AB} magnitude is listed in column 4, followed by I, V and K three-arcsec aperture magnitudes, measured redshifts, 'galaxy type', radio spectral indices and $[\text{O II}]$ (rest) equivalent widths. The 'galaxy types' given in the table represent broad divisions on the basis of their spectra, colour indices and morphologies (see below) into ellipticals (E), post-starburst (S+A – see section 3.3), and emission-line galaxies (EM). Question marks appended to these 'types' indicate that the classification was based on colours and radio properties. Note that several of the sources in the FWKK 'complete' sample (with 8 arcsec resolution) are actually blends of sources which are resolved at their highest resolution ($2''.5$, 4.8GHz). In most cases, each of these individual radiosources were also identified with optical counterparts. However, since some of these resolved sources have no individual sources with flux higher than $16 \mu\text{Jy}$, they should not be included in the complete subsample. The five sources listed at the bottom of Table 1 are in this category. After these sources have been removed (and one double source counted as two), the complete sample in our MOS field is reduced to 36 radio sources, almost all of which are unresolved, even at FWKK's highest resolution. Only two radio sources (15V62 and 70) remain unidentified, even in the sum of our deep optical images from the B to the K band. The resulting completeness in optical identification is 94 per cent.

The positional offsets and discussions of the identifications of the objects are given in the notes to Table 1, and

Table 1. Optical Counterparts of μ Jy Sources

Objects with $S > 16\mu\text{Jy}$ and $I_{AB} \leq 22.5$												
FWKK	S	CFRS	I_{AB}	I(3")	V(3")	K(3")	z	Type	α	err	$W_{[OII]}$	err
15V..	μJy	14..	mag	mag	mag	mag					\AA	\AA
5	41	1501	21.74	22.04	23.16			S+A?	0.2	0.3		
10	1912	1373	21.77	22.27	24.55	20.56		E?	<-0.2	0.1		
11	70	1329	19.49	19.86	20.94		0.375	S+A	0.5	0.1	15	5
12	45	1303	19.97	20.14	20.05	19.25	0.985	QSO	0.1	0.3	30	3
15	24	1246	22.18	22.30	23.92			E?	<-0.3			
19	24	1190	20.99	21.17	22.67		0.754	S+A	0.7	0.3	10	3
21	298	1177	20.78	21.29	22.68		0.724	S+A	0.3	0.1	68	20
23	54	1157	20.54	21.08	22.99		1.149	?	0.3	0.2	33	10
24	79	1139	20.20	20.64	21.93	18.92	0.660	S+A	0.4	0.1	16	4
26a	47	1041	21.7	21.87	22.36		0.372	EM	<-0.1		75	7
26b	47	9025	18.31	19.27	20.04		0.155	EM	<-0.1			
28	31	1028	21.57	21.74	24.01	19.69	0.988	E	-0.3	0.6	31	15
34	1311	0937	21.41	22.01	24.42		0.838	E	<-0.2		12	8
39	35	0854	21.7	21.85	24.08	19.59	0.992	E	-0.8	0.7		
40	33	0820	21.69	21.94	24.52	19.37	0.976	E	-0.1	0.4	24	12
42	14	0727	20.62	21.05	21.90		0.463	EM			40	8
47	53	0665	22.41	23.00	23.67	21.93		?	0.5	0.2		
48	20	0663	20.88	21.11	22.57		0.743	S+A	0.2	0.4	11	4
49	31	0667	19.48	19.96	20.65	18.92		?	0.7	0.3		
50	705	0645	22.44	22.76	24.72			?	0.7	0.1		
57	37	0573	16.90	17.70	17.89	17.53	0.010	EM	<-0.5			
60	39	9154	21.57	21.94	23.43		0.812	S+A	0.3	0.2	75	30
65	35	0426	19.80	19.86	21.48		0	M*	0.4	0.4		
73	37	0276	20.67	20.95	22.93		0.746	E	<-0.5			
81	28	0154	22.08	22.16	22.74		1.158	EM	0.7	0.2	55	10
Objects with $S > 16\mu\text{Jy}$ and $I_{AB} > 22.5$												
FWKK	S	CFRS	I_{AB}	I(3")	V(3")	K(3")	z	Type	α	err	$W_{[OII]}$	err
15V..	μJy	14..	mag	mag	mag	mag					\AA	\AA
18	44			> 25	> 26	20.8			0.2	0.3		
33	20	9991	23	23.2	24.7			E?	<-0.2			
37	51	0861	23.5	23.65	25.25	20.23		E?	-0.4	0.4		
45	33	9993	24.1	24.3	> 26			E?	-0.2	0.7		
51	41	9994	22.99	23.14	> 26				0.4	0.2		
53	30	0612	23.0	23.04	23.95			S+A?	0.7	0.2		
59	19	9995	24.3	24.5	24.4				0.1	0.5		
62	24			> 25	> 26	> 21			<-0.3			
67	46			> 25	> 26				-0.3	0.3		
70	576			> 25	> 26				0.6	0.1		
72	32	9996	23.6	23.8	> 26	20.6		E?	-0.5	0.5		
Objects with $S < 16\mu\text{Jy}$ after deblending of the radio emission												
FWKK	S	CFRS	I_{AB}	I(3")	V(3")	K(3")	z	type	α	err	$W_{[OII]}$	err
15V..	μJy	14..	mag	mag	mag	mag					\AA	\AA
30	< 26	0983	21.27	21.53	21.84	20.79	0.286	EM	0.9?	0.2	58	15
30	< 26	0998	20.58	20.73	21.99	19.06	0.43		0.9?	0.2	18	4
36	< 22	0887	20.46	20.69	22.16				0.2	0.5		
41	< 38	0818	21.02	21.33	22.45		0.899		-0.4	0.8	39	10
69	13	0393	20.44	20.66	21.64	19.76	0.602		-0.3	0.5	36	8

the radio positions are also indicated on images of all the 40 sources that lie in the field in Fig. 1.

2.5 Notes on individual sources

15V5: Excellent positional agreement ($0''.1$) with CFRS-14.1501 but no spectrum was obtained.

15V10: CFRS14.1373 is slightly offset ($1''.6$) from the radio core of this extended double source as shown in the map by FWKK, but it appears to be the probable identification. An uncertain redshift of 0.652 was derived, but no [O II] emission, characteristic of most of these radio sources, is detected.

15V11: Excellent positional agreement ($0''.5$) with CFRS-14.1329.

15V12: Excellent positional agreement ($0''.4$) with CFRS-14.1303, a quasar at $z = 0.985$ associated with a large structure of galaxies (Le Fèvre et al. 1994) in this field.

15V15: Only fair positional agreement ($2''.0$) with CFRS-14.1246 for which we derive a tentative redshift of $z = 0.65$. FWKK claim it is “at edge of galaxy with a double nucleus”, but the faint objects shown in Fig. 1 appear to be isolated galaxies.

15V18: Nothing visible at the radio source position on the summed B, V and I image, but a faint counterpart is visible on the K image. It is thus extremely red, $(I - K)_{AB} > 4.4$, and probably at $z > 1$.

15V19: Excellent positional agreement ($0''.2$) with CFRS-14.1190.

15V21: Poor positional agreement ($4''.6$) with CFRS14.1177 which has $z = 0.724$. Although the spectrum of this galaxy shows [O II] emission, typical of the optical counterparts, it appears that the fainter ($I_{AB} \sim 23.9$) galaxy which is only $2''.0$ away is a more likely counterpart. FWKK comment that a source 13 arcsec E confused the map of this source, possibly the explanation of the poor positional agreement. Unfortunately, no spectrum of the fainter galaxy was obtained.

15V23: Excellent positional agreement ($0''.4$) with CFRS-14.1157, a galaxy with a peculiar morphology and a peculiar red spectrum displaying strong emission at 8008\AA identified as 3727, and possibly other weaker emission lines at this redshift. We adopted $z = 1.149$ as the most likely redshift, but $z = 0.372$ cannot be ruled out. If it is at the high redshift, it is similar in some respects to the well-known powerful radiosources at similar redshifts.

15V24: Excellent positional agreement ($0''.6$) with CFRS-14.1139.

15V26: According to FWKK, the radio emission comes from both the bright spiral galaxy (CFRS14.9025) and the fainter galaxy (CFRS14.1041) to the east. The latter object shows strong [O II] and [O III] emission lines; the brighter one shows strong $H\alpha$ and [SII] emission.

15V28: Excellent positional agreement ($0''.7$) with CFRS-14.1028. FWKK give $31\mu\text{Jy}$ for the radio emission of the “core” associated with this galaxy, and comment that the extended emission (see their map) may come from other galaxies.

15V30: There are two radio lobes, each centered on a galaxy; the northern one (CFRS14.983) is a strong emission line object at $z = 0.286$, and the other (CFRS14.0998) has a more normal spectrum.

15V33: The radio source appears to be associated with a faint red galaxy.

15V34: There is excellent positional agreement ($0''.3$) of this strong radio source with CFRS14.0937.

15V36: Although the position of this radio source is $3''.7$ away from CFRS14.0887, the FWKK radio map shows that there is a radio lobe centered on it (but with $S < 16\mu\text{Jy}$).

15V37: There is a very faint ($I_{AB} \sim 23.5$) galaxy coincident with this source (offset $0''.5$) but no spectrum was obtained.

15V39: Excellent positional agreement ($0''.5$) with CFRS-14.0854, a galaxy at $z = 0.992$ which has a faint ($I_{AB} \sim 23.2$) companion only $2''.1$ away.

15V40: The positional agreement ($0''.8$) with CFRS14.0820 is good.

15V41: Although CFRS14.0818 ($z = 0.899$) is $3''.5$ W of the catalogued position of this radio source, the highest resolution map given by FWKK shows a source coincident with this galaxy, and they comment that the radio source is probably a blend of emission from several galaxies (with $S < 16\mu\text{Jy}$). In addition, the spectrum shows strong [O II] emission and strong Balmer absorption lines indicating on-going star formation.

15V42: The radio source is located rather far away ($2''.5$) from the centre of CFRS14.0727, a large galaxy at $z = 0.463$, and hence may not be associated with it at all. However, the spectrum of this galaxy shows strong [O II] and [O III] emission indicating that it probably is the radio source.

15V45: There is a very faint ($I_{AB} \sim 24.3$) galaxy coincident with this radio source, but it is not visible on our V image.

15V47: A spectrum of the brightest part of CFRS14.0665, the nearest (~ 2 arcsec away) galaxy (or galaxies?) to the radio source was obtained, but no features were unambiguously identified, possibly indicating a high redshift.

15V48: Excellent positional agreement ($0''.2$) with CFRS-14.0663.

15V49: Although the catalogued position for this radio source is $1''.9$ away from CFRS14.0667, the highest resolution radio map shows a source coincident with it. Unfortunately, no spectrum was obtained, but the extended appearance of the galaxy suggests that $z \lesssim 0.5$ rather than $z \gtrsim 1$.

15V50: Excellent positional agreement ($0''.4$) with CFRS-14.0645 but no spectrum was obtained.

15V51: Excellent positional agreement ($0''.4$) with a faint red galaxy.

15V53: Good positional agreement ($1''.1$) with CFRS14.0612 but no certain features were identifiable on our rather poor spectrum.

15V56: This source lies within the visible extent of a bright nearby spiral (CFRS14.0573; radio source 57). No distinct object is visible on our images at the location of the source, but since it is effectively masked by the bright foreground galaxy, it was removed from our complete sample.

15V57: Excellent positional agreement ($0''.6$) with CFRS-14.0573, a bright $z = 0.010$ galaxy displaying a strong starburst spectrum.

15V59: This source is coincident with a very faint galaxy. The bright object $3''.9$ E is an M star.

15V60: Excellent positional agreement ($0''.3$) with CFRS-14.9154.

15V62: Nothing visible on any of our images (even summed) at the location of the source.

15V65: Despite the apparent discrepancy ($1''.4$) between the position of CFRS14.0426 and the catalogued radio position, the highest resolution map published by FWKK shows a source coincident with CFRS14.0426, an M star.

15V67: No optical counterpart of this compact source is visible on our I image, but a very faint object is present (at $V \sim 24.7$) on the sum of our B, V, and I images. Unfortunately, we do not have a K image.

15V69: Excellent positional agreement ($0''.2$) with CFRS-14.0393, but FWKK comment that the core associated with

Figure 1. Finding charts for all the 40 FWKK sources identified in the CFRS MOS field. The areas shown are $20''.7 \times 20''.7$ with N at the top and E to the left, and they were extracted from a combined B, V and I image (except for 15V18 which was identified on a K image). The radio positions are marked either by a cross or by a circle.

this galaxy is $13\mu\text{Jy}$ and that there is an extension to the E responsible for the remaining $10\mu\text{Jy}$.

15V70: Nothing visible on any of our images, including the sum of B, V and I, at the location of the source. No K image was taken.

15V72: The core ($32\mu\text{Jy}$ according to FWKK) is apparently coincident with the faint galaxy located $\sim 1''.5$ SW of the cross shown in Fig. 1 and is presumably identified with it. The bright object $4''.3$ E of the quoted radio source position, CFRS14.0274, is an M star.

15V73: Good positional agreement ($0''.8$) with CFRS14.0276, one of the few optical counterparts which does not have [O II] emission.

15V81: Good positional agreement ($0''.7$) with CFRS14.0154, a galaxy for which we derive $z = 1.158$ based on one strong emission line assumed to be 3727 [O II].

3 NATURE OF THE SOURCES WITH $I_{AB} < 22.5$

3.1 Morphological and photometric properties

Most of the sources show typical morphologies for galaxies, i.e., round, edge-on disk, or irregular shapes. Only two sources (the quasar 15V12 and the M star 15V65) are not spatially resolved, while some sources show compact cores.

Figure 2. Morphologies of some optical counterparts before and after deconvolution for (see text): a) 15V23, I; b) 15V47, I; c) 15V49, I; d) 15V 26a and b; e) 15V18, K.

Figure 3. Histogram of the μJy radio source optical counterparts in a) V band; b) I band. A limit of $V=26$ and $I=25$ have been adopted for the undetected sources.

Deconvolution demonstrates that three sources (15V23, 47 and 49) present very complex morphologies with more than three individual components within 2 arcsec (see Fig. 2). These components appear to have very different colours one from another, and it is difficult to understand the nature of these peculiar sources from our data.

Histograms of the V and I magnitude distributions are shown in Fig. 3 for all sources of the complete sample, assuming that the two unidentified sources have $V_{AB} > 25$ and $I_{AB} > 24$ respectively. The V histogram (Fig. 3a) shows the expected increase of the source number with magnitude, until the magnitude limit is reached. However, the I histogram (Fig. 3b) has a well-defined peak at $I_{AB} = 21.9$, much brighter than our completeness limit.

3.2 Redshifts

The spectra of all objects which we observed are shown in Fig. 4. Secure redshifts were determined for 19 of the counterparts, and less reliable redshifts for two more (15V10 and 15V15), but no redshift could be determined for 15V47. Spectroscopic observations were also made of 4 of the coun-

Figure 4. Spectra of 19 μJy radio source counterparts which resulted in secure redshift identifications.

terparts which we subsequently rejected because their deblended radio flux was too low, and a spectrum was obtained of the very faint counterpart of 15V53, but we were unable to determine its redshift. The completeness of our redshift determinations of objects with $S > 16\mu\text{Jy}$ and $I_{AB} \leq 22.5$ is 86 per cent, identical to that for the CFRS survey as a whole.

The main spectroscopic properties of the sources are listed in Table 1. In the double-limited sample, there is one M star (15V65), one QSO (15V12) and one overluminous ($\sim 10L^*$) galaxy at $z = 1.149$ (15V23) which was already noted to have a very complex morphology. The rest of the sources can be divided into three different classes from their colour and spectral properties and include 5 very blue emission-line galaxies (26 per cent of the whole sample), 6 spirals (32 per cent) and 5 ellipticals (26 per cent).

3.3 Optical spectra and colours

The 5 emission-line galaxies (15V26a, 26b, 42, 57 and 81) have generally blue V-I colours and are distributed over a large range in redshift and absolute magnitude (Figures 5a and b). At first sight these spectra resemble those of starburst galaxies which Benn et al. (1993) claim to be common at 0.1 mJy levels. However, detailed analyses of the spectra suggest that their ionisation sources may be more closely related to those in AGNs. We have quantified the emission line activity in these galaxies by measuring their line ratios and plotting them in the diagnostic diagrams developed by Veilleux and Osterbrock (1987). 15V57 has $\log([\text{S II}]/\text{H}\alpha) = -0.41$ and $\log([\text{O III}]/\text{H}\beta) = 0.83$, which together with the presence of $[\text{O I}]630.0$ definitely indicates this object is a Seyfert 2 galaxy (Fig. 4). This object has the lowest redshift of our sample ($z = 0.01$) and would be classified as a dwarf blue elliptical from its luminosity, colour and morphology. 15V26b is not as blue as the other ones (its V-I colour suggests a Sa galaxy), but it has an emission line spectrum characteristic of a LINER ($\log([\text{S II}]/\text{H}\alpha) = -0.32$, $\log([\text{N II}]/\text{H}\alpha) = -0.26$, with no $[\text{O III}]$). It is located in a large edge-on disk (Fig. 2d). 15V26a and 15V42 have both $[\text{O II}]3727$, $[\text{O III}]5007$ and $\text{H}\beta$, which also allows classification of their ionisation source (see Tresse et al. 1994).

Figure 5. a) Hubble diagram for the spectroscopically identified sources. Curves are (k-corrected) redshift magnitude relations for L^* galaxies (early types to later type), derived from Bruzual and Charlot (1993) models. Symbols are filled circles for early type galaxies (E/S0), filled squares for later type galaxies ($\sim\text{Sa}$ to Sbc), filled triangles for emission-line galaxies and stars for other peculiar objects. b) V-I versus redshift diagram. Symbols and curves have the same meaning as in Fig. 5a).

The line ratios are $\log[\text{O III}]/\text{H}\beta = 0.72 \pm 0.4$, 0.58 ± 0.2 and $\log[\text{O II}]/\text{H}\beta = 0.95 \pm 0.3$, 0.76 ± 0.2 respectively for 15V26a and 15V42. Although the errors are relatively large, to provide such intensity ratios requires high temperature ionisation sources ($T \sim 100\,000\text{K}$), more characteristic of an AGN than massive stars. Furthermore, we have not been able to estimate the extinction, so the calculated $[\text{O II}]/\text{H}\beta$ ratios are underestimates.

15V26a has an irregular morphology (Figure 2d), while 15V42 is a nearly edge-on disk galaxy, and both have luminosities substantially lower than L^* . The source with the highest redshift among these objects is a very blue emission-line galaxy (15V81, $z=1.158$) which is brighter than L^* . We have no real indication of the nature of this object since most of the emission lines are outside our spectroscopic window.

Six galaxies (11, 19, 21, 24, 48, 60) have spiral-like characteristics, with colours ranging from Sa to Sb, and disk-like morphologies. They are rather luminous galaxies ($L \sim 1.5 \pm 0.4L^*$) and lie at moderately high redshift (from $z = 0.37$ to $z = 0.81$, average $z = 0.6$). They all show moderate $[\text{O II}]$ emission (average $W = 12\text{\AA}$ at rest), and relatively strong Balmer continuum and absorption lines. These features are easily seen in the combined spectrum (Fig. 6a). Equivalent widths of the Balmer absorption lines range from 3 to 5\AA , indicating the presence of A and F stars suggesting that strong star formation occurred in these objects ~ 1 Gyr ago. In addition, strong $[\text{O II}]$ emission is present in the spectra of these galaxies and so we classify them as ‘S+A’ galaxies by analogy with the E+A galaxies described by Dressler & Gunn (1983).

The spectra of five of the galaxies (28, 34, 39, 40, 73) are more typical of ellipticals, with well-defined 4000\AA breaks and faint or no $[\text{O II}]$ emission lines ($W = 3.5\text{\AA}$ at rest from the combined spectrum, Fig. 6b). Their V-I colours are bluer than old and non-evolved stellar populations by ~ 0.7 mag-

Figure 6. a) Summed spectra of 6 galaxies classified as S+A (poststarburst) on the basis of their spectral features, colours and morphologies. Note the strong Balmer absorptions and continuum which almost hide the 4000Å break. b) Combined spectra of the 6 galaxies classified as early-type galaxies.

nitude. They are luminous galaxies ($L \sim 1.9 \pm 0.2 L^*$) and lie at higher redshifts (0.75 to 0.99) than the ‘S+A’ galaxies.

3.4 The radio spectral index–colour diagram

Figure 7 shows the radio spectral index α between 1.5 and 5GHz for each identified object (filled points) in our sample, versus their V-I colour. Each of the three μ Jy populations occupy distinct areas in the diagram: all red ellipticals have inverted radio spectra ($\alpha = -0.4 \pm 0.3$), all the S+As have moderately steep spectra ($\alpha = 0.40 \pm 0.18$), while the bluest emission-line galaxies have inverted spectra, with the notable exception of the most distant one, 15V81 ($\alpha = 0.7$). Inverted-spectrum radio emission from ellipticals has been observed in some nearby ellipticals (Wrobel and Heeschen 1984). According to Rees (1984), this may indicate the presence of a low-power AGN, although other alternatives are possible. It is unlikely that the observed inverted radio spectra can be attributed to opacities at low frequencies since it only affects emissions below 1GHz at rest (see Condon 1992), i.e., below 0.5 GHz at $z \sim 1$.

Inverted radio spectra are also exhibited by the four very blue galaxies at low and moderate redshift, supporting the hypothesis that AGNs are present in their cores too, producing both the radio emission and the emission lines. Note also that the QSO (15V12) lies in the area of blue emission-line sources in Fig. 7.

The post-starburst spirals have radio slopes noticeably flatter than the mJy starburst galaxies, which might indicate an increasing contribution of thermal radiation from remnant supernovae (Condon 1992). The radio emission from 15V81 could be ascribed to star formation similar to that from starbursts observed at higher radio fluxes. Finally, the source 15V23 is more difficult to interpret, since it has a positive radio index and there is some uncertainty about its true V - I colour because of its complex optical morphology.

Figure 7. The radio spectral index versus V - I colour for all objects in the complete sample. The symbols are the same as in Figure 5, except that open circles represent the faintest optical counterparts without spectral classification. The FWKK number of each source is given beside each symbol, and the arrows denote limits. Note the location of the early-type galaxies in the bottom right, the S+As (post starburst) in the middle top and the emission-line objects either in the top left (one starburst, 15V 81) or in the bottom left (AGN induced emission-line galaxies). Note that the low V-I values for the latter objects are also due to their moderate redshift. Delimiting areas are indicated from the location of spectroscopically-identified objects, separating the early type galaxies (E/S0) from the post starburst galaxies (S+A). An extension of the E/S0 area is also indicated for large redshift where V-I is likely to decrease. A typical error bar is shown at lower left.

3.5 $I_{AB} < 22.5$ objects with no redshifts

Among the 25 $I_{AB} < 22.5$ optical counterparts, we failed to get secure redshifts for 3 of them, while for observational reasons we were not able to observe three others. There is some indication that the three spectroscopic ‘failures’ (15V10, 15 and 47) all lie at $z > 1$. In the V - I - spectral index diagram, 15V10 lies in the area defined by ellipticals with low power AGN, while 15V15 is slightly offset to bluer colour, as expected if it is at $z > 1$. 15V47 has a very complex morphological type which leaves some uncertainty in the colour of its optical counterpart; it may be similar to the high z object 15V23. Hence it is possible that we failed to get good redshifts for these objects simply because their dominant spectral features ([O II] 372.7 nm and 400.0 nm break) are beyond our spectroscopic window ($> 8500\text{Å}$), resulting in featureless spectra (Fig. 4).

The three objects for which we do not have spectra (15V5, 49 and 50) all have relatively steep radio spectra. 15V5 is likely to be an S+A galaxy from its location in Fig. 7 and from its elongated morphology. 15V49 has the most complex morphology of our sample, while the nature

Figure 8. V-I versus I-K colour indices. Typical evolutionary tracks are shown for three classes of galaxies (solid lines), with three fiducial redshifts marked by dashed lines. As before, spectroscopically-classified objects are represented by filled symbols, objects without redshifts by open symbols. There are three faint objects which show definite high I-K colours, which are likely to be early-type galaxies at $z > 1$.

of 15V50 is not clear, since it has a red colour and a steep radio slope.

4 NATURE OF THE $I_{AB} > 22.5$ COUNTERPARTS

The fact that we have redshifts and colours and hence have been able to determine the nature of most of the sources with $I_{AB} < 22.5$, allows us to extend our analysis to the fainter sources, using only their colours and spectral indices. Among the 11 $I_{AB} > 22.5$ sources, two have no optical counterparts and one is only detectable in the combined B+V+I image, so it is impossible to speculate on the nature of these.

There is considerable evidence that virtually all of the remaining sources are likely to be at $z > 1$. Four of them, 15V33, 37, 45 and 72, have properties similar to the high redshift early-type galaxies. In fact, the two for which we have K photometry have colours much redder ($I-K = 3.4$ and 3.2 for 15V37 and 15V72 respectively) than any object in the CFRS sample ($I_{AB} \leq 22.5$). This, their round morphologies, and their V-I colours (Fig. 8) are all consistent with early-type galaxies at $z > 1$. The reddest source of our sample is 15V18, with $I-K > 4.2$. Its morphology is surprisingly elongated, similar to that of an edge-on disk (Figure 2). If this is the case, this source might be a late-type galaxy at redshift even larger than 2. The location of 15V53 in Fig. 7 supports identification with a S+A galaxy, very probably also at $z > 1$, from its faintness and its colour. 15V59 is located near the QSO (15V12) in Fig. 7, and hence might be either a QSO or an AGN-powered source. After deconvolution, 15V59 appears to be composed of two compact components. 15V51, which has an elongated morphology, appears to be similar to 15V50 and is also a candidate to be a radio galaxy at very high redshift.

5 THE MICROJY RADIO SOURCES

Combining the results from the two previous sections, an estimate can be made of the relative contribution of the different types of objects to the μJy population. We then find, among the 36 FWKK radio sources with $S > 16\mu\text{Jy}$ in our MOS field:

- 5 definite and 6 probable early-type galaxies (~ 33 per cent of sample). The latter 6 are probably at $z > 1$.

- 7 S+A's (21 per cent) including 1 possibly at $z > 1$.

- 7 blue emission line objects (21 per cent), including 1 (or 2) QSOs.

- 3 sources (9 per cent) with a very complex optical morphology, including one at $z = 1.15$.

- 2 candidates for very high redshift radiogalaxies.

- 1 very elongated object with colours consistent with location at very high z .

- 1 starburst at $z = 1.135$.

- 1 M star.

- 3 undetected or barely detected objects.

The microJy population is hence mainly constituted of three distinct populations of galaxies with different redshift regimes: early-type galaxies at $z > 0.75$, S+A at intermediate redshifts ($z = 0.375$ to $z = 0.8$ or slightly > 1), and emission-line galaxies at $z < 0.45$ containing AGNs.

It is possible that the early-type galaxies may be over-represented, since three of the spectroscopic identifications belong to the structure at $z = 0.985$ found in this field (Le Fèvre et al. 1994), and it is not clear whether this has any effect or not. The fraction of μJy sources with $z > 1$ is 38 - 42 per cent, depending on whether one assumes the unidentified sources are all at high z , or if they have the same distribution as the rest of the sample.

6 DISCUSSION

6.1 Comparison of μJy with sub-mJy sources

At bright flux levels near ~ 1 mJy, the radio source population is known to be composed largely of starburst galaxies at moderate redshifts. However, even though it is believed that this may continue to the sub-mJy levels, no spectroscopic sample as complete as the one presented here has yet been gathered. Thuan and Condon (1987) have shown that optical-infrared colours of sub-mJy radiosources are similar to that expected for Irr or starbursting galaxies, and Rowan-Robinson et al. (1993) have discussed their evolution, but conclusions are limited by the low identification rate (112 of 523) of the sources. Benn et al. (1993) were only able to identify the brightest ($B < 22.3$) optical counterparts and may have missed most of the $z > 0.5$ identifications (see Colless et al. 1990). Windhorst, Dressler and Koo (1987) also obtained spectra for a small sample of only ~ 10 sub-mJy radiosources, all of which show [O III] and $H\beta$ lines with $W \sim 20-30\text{\AA}$.

Our data indicate that the star formation activity, as well as the corresponding radio power, may decrease towards lower flux limits. Only one galaxy in our sample has a classical starburst spectrum, and it is at a much higher

redshift than the Benn et al. sources. As noted above, most of the emission-line galaxies identified by us appear, from their emission line ratios and from their inverted or flat radio spectra, to be powered by AGN rather than starbursts. On the other hand, the S+A objects in our sample may well be the remnants of an active starburst population. Starburst activity is expected to last for only a relatively short period (typically 10^8 yrs), followed by a decrease in radio and emission line activity which in turn produces a less steep radio spectrum (increasing contribution from the thermal radiation by supernovae remnants) and optical spectra dominated by several Gyr old stars (A and F stars), with faint [O II] and no [O III] emission. The surface density of the S+A post-starburst population found at μJy levels – assuming the count slope of 1.18 from FWKK – is indeed ten times larger than that of the mJy population at 1.4GHz, which is assumed to be mainly composed of starbursting galaxies. It is thus possible that the S+A galaxies are the remnants of generations of active starburst galaxies.

6.2 Radio emission from distant ellipticals compared to nearby ones

The presence of radio emission in a large fraction of nearby early-type galaxies is well known, and has been widely studied by Wrobel and Heeschen (1991) in a complete survey at 6cm. They found that ~ 30 per cent of nearby ellipticals have radio emission in their cores at powers ranging from 10^{19} to 10^{21} W Hz $^{-1}$, which are believed to be linked with low-power AGNs, since the core radio emission of a small subsample have flat or inverted radio spectra. The radio emission from the high redshift early-type galaxies in our sample probably has the same origin, since for all but one (15V10), the radio emission is concentrated in regions smaller than $0''.2$ to $2''$. However, at $z > 0.75$, more than a third of the early-type galaxies have $P > 10^{23}$ W Hz $^{-1}$, much larger than those in the Wrobel and Heeschen sample. The samples are not directly comparable, however, since only 4 of their galaxies have comparable optical luminosity to those in our sample, and their radio power is more than ten times lower.

It is thus more relevant to compare our results to higher flux limit surveys. In the Parkes sample (Wall et al, 1971; Downes et al, 1986; Dunlop et al. 1989), at the flux limit of $S_{2.7\text{GHz}} = 100\text{mJy}$, no flat spectrum radio galaxy was found below $z = 0.02$, the redshift at which a 10^{23} W Hz $^{-1}$ source is at the Parkes flux limit. We find 5 flat spectrum ellipticals ($0.75 < z < 1$) in the volume contained in our $10' \times 10'$ MOS field, which is 7.5 times smaller than the volume in the Parkes survey to $z = 0.02$. Dunlop et al. (1989) found one similar source at $z = 0.118$, PKS 1215+013 ($P=5 \times 10^{24}$ W Hz $^{-1}$ and $\alpha = -0.15$), but again the corresponding volume is more than 1000 times larger than our CFRS volume. Note that the bulk of the galaxy population sampled in the CFRS lies at $z = 0.3$ to 1.

We thus conclude that radio flat spectrum sources ($P \sim 5 \times 10^{23}$ W Hz $^{-1}$) occur much more often in high redshift early-type galaxies than in low redshift ones. The fact that the fraction of radio emitting early-type galaxies in the μJy population is increasing with the redshift (0 per cent at $z < 0.5$, 25 per cent at $z < 1$ and 40 per cent at $z > 1$)

also demonstrates that early-type galaxies are experiencing strong evolution of their radio properties beyond $z = 0.75$. Indeed, one third of them apparently exhibit AGN activity at $z \sim 1$. One cautionary note must be added however, since Le Fèvre et al. 1994 detected a large structure at $z \sim 1$ in this field, and so it is conceivable that this field may be unusual.

7 CONCLUSION

During the course of the CFRS project we have observed 36 μJy radio sources which form a complete subset of the FWKK sample ($S_{5\text{GHz}} > 16\mu\text{Jy}$). Optical counterparts have been identified for 94 per cent of these, and redshifts have been determined for 86 per cent of those with $I_{AB} < 22.5$. Among the latter, which are mainly at $z < 1$, three different populations of comparable weight (from 26 to 32 per cent) are identified: emission-line galaxies whose activity resembles that in AGNs, luminous post-starburst spirals containing many A or F stars, and high redshift luminous early-type galaxies containing low-power AGNs.

Based on our knowledge of the redshifts, colours and radio spectral indices of the brighter objects, we are able to extend our analysis to all sources in the radio flux-limited sample. We find that 40 per cent of the total sample μJy radio sources probably lie at $z > 1$, and nearly half are early-type galaxies.

The fact that blue galaxies with emission lines in our sample also have inverted radio spectra is additional evidence that low-power AGNs may reside in their cores, in accord with the results at lower redshift discussed by Tresse et al. 1994. We also postulate that the S+A galaxies in our sample may be the result of evolution of starbursting galaxies to a more quiescent state, as indicated by both their radio emission and optical emission lines, since their surface density is consistent with that of mJy starburst sources. The sources corresponding to luminous early-type galaxies, a population which represents an increasing fraction with redshift (40 per cent at $z > 1$), also frequently appear to contain a low-power AGN nuclear source. Although Wrobel and Heeschen (1991) report similar radio activity in ellipticals at low redshift, they have much lower radio power.

The mixture of the three dominant populations in the μJy counts explains the apparently discrepant V and I histograms of their optical counterparts. Red early-type galaxies at high redshift contribute to the $I_{AB} = 21.9$ peak, but they have very faint V magnitudes. The strong decrease of the radio spectral index from sub-mJy to μJy counts appears to be due to a combination of three factors: (1) the emergence of an elliptical population at high redshifts with moderate radio emission (2) an increasing fraction of narrow emission-line AGNs (Seyfert 2 and LINER); (3) a higher contribution of the thermal radiation to the radio emission from spirals, and the almost complete disappearance of starburst galaxies. The fact that radio sources have much flatter radio spectra at μJy levels compared to those above 0.1 mJy can thus be mostly attributed to the emergence of radio sources driven by low-power AGNs (> 50 per cent of the whole μJy population). Since the space density of AGN-driven sources apparently overtakes those powered by stellar emission, the

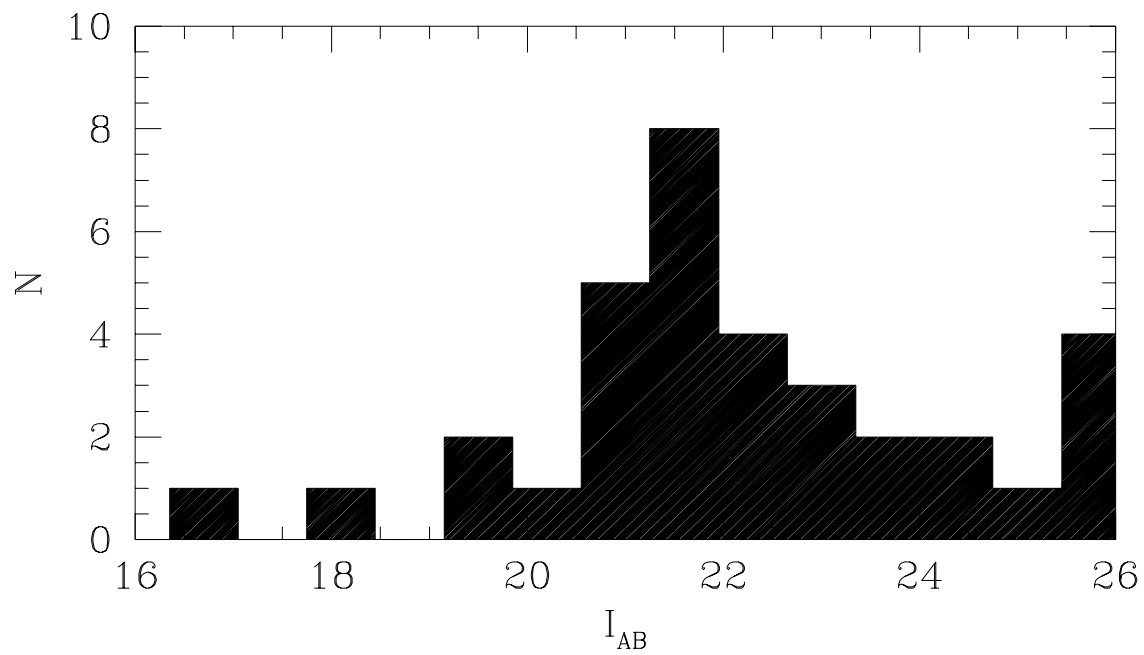
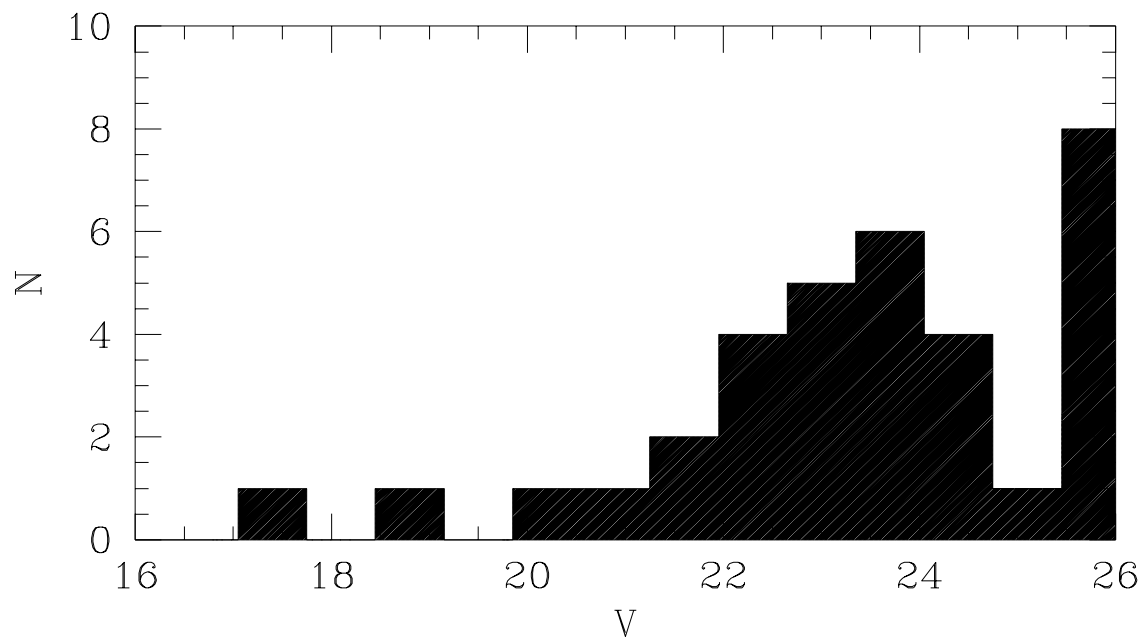
contribution of AGN light to the faint source counts should be reevaluated. Finally, our results demonstrate that a similar study of a complete sample at sub-mJy levels should be carried out, as well as an extension of the present survey to other fields surveyed at μ Jy depth.

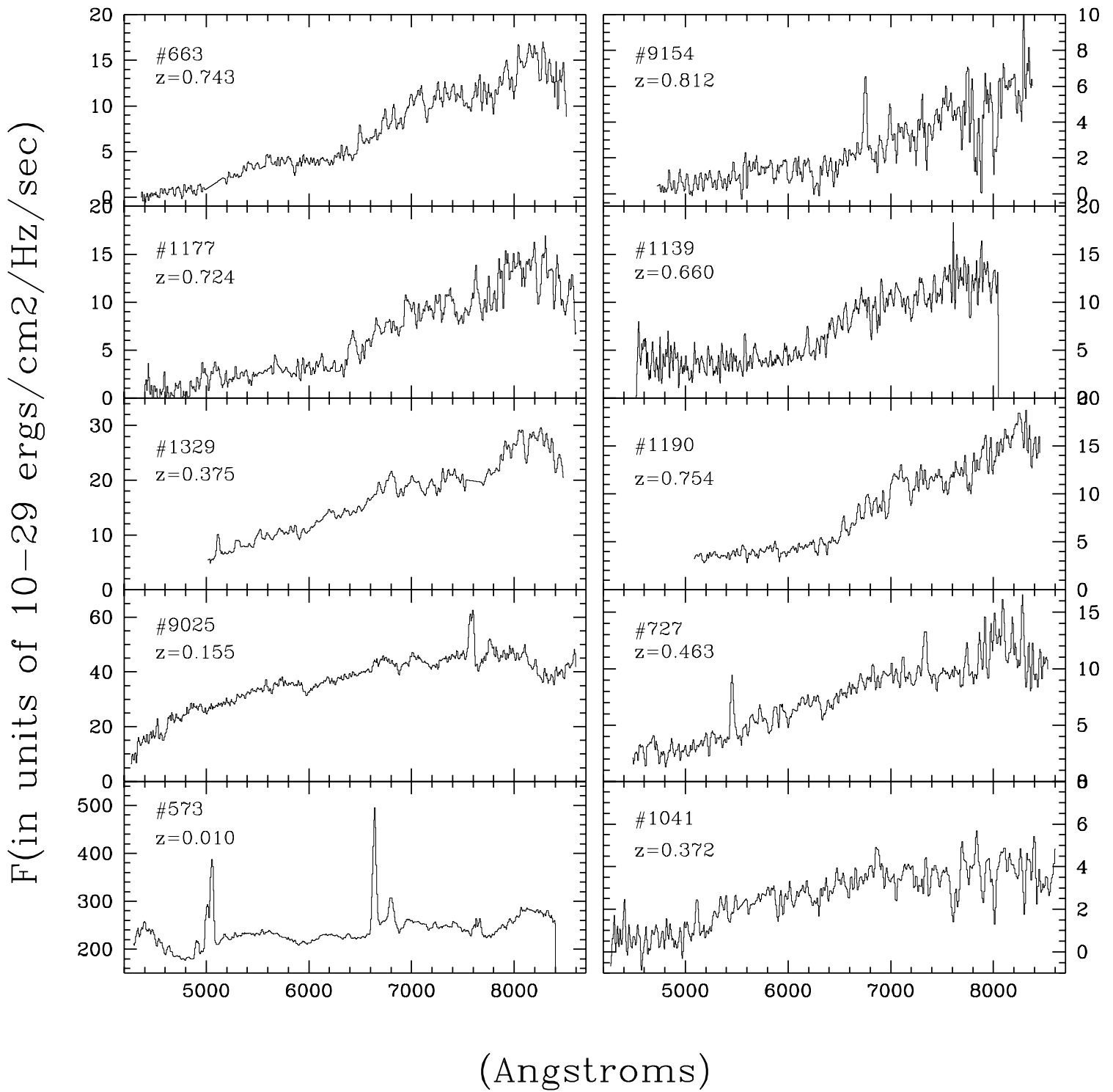
ACKNOWLEDGMENTS

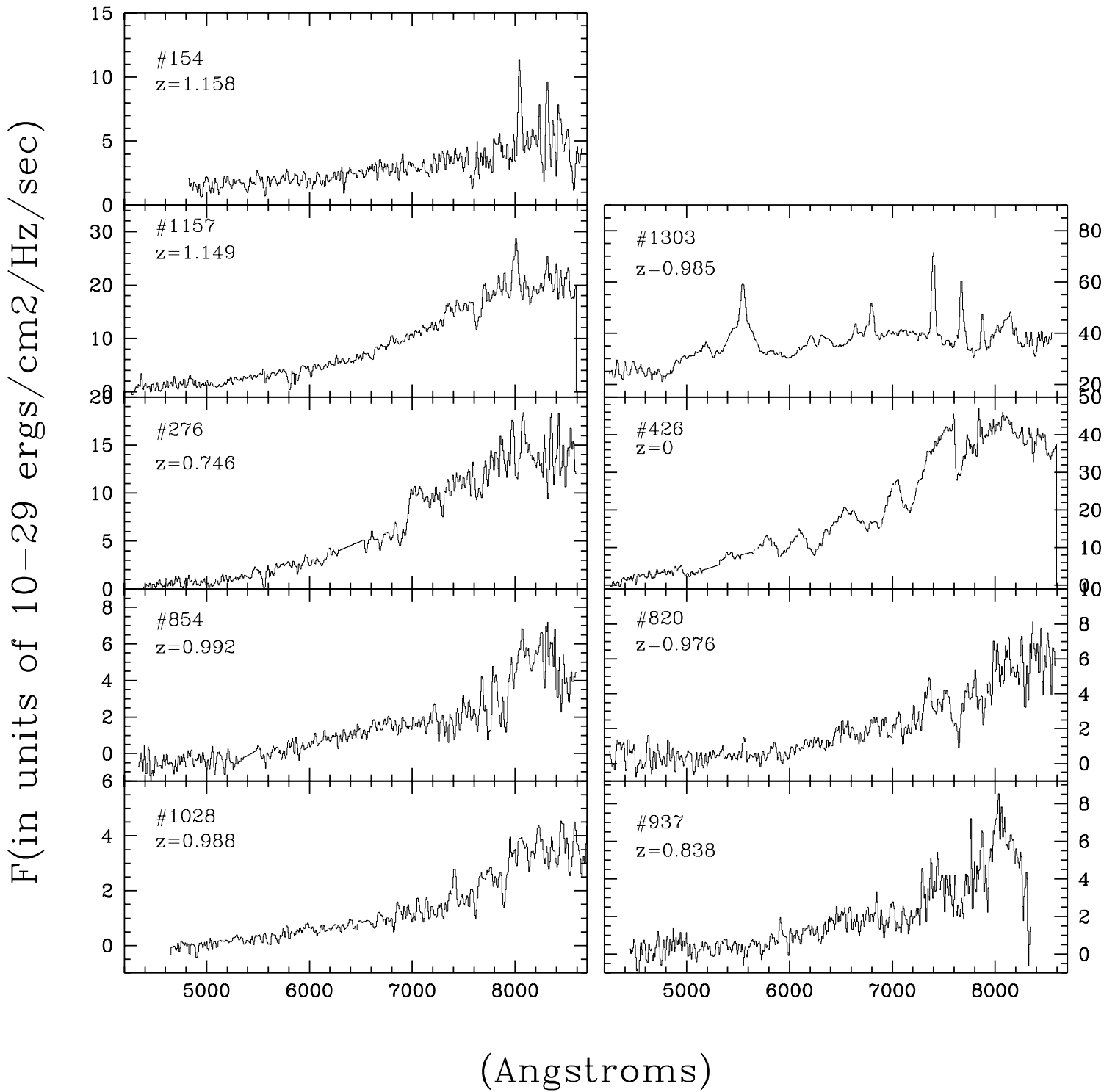
We thank J. Kristian and R. Windhorst for discussions, the referee, J. Wall for helpful comments and the directors of the CFHT for their continuing support and encouragement. SJL's research is supported by the NSERC of Canada. We acknowledge some travel support from NATO.

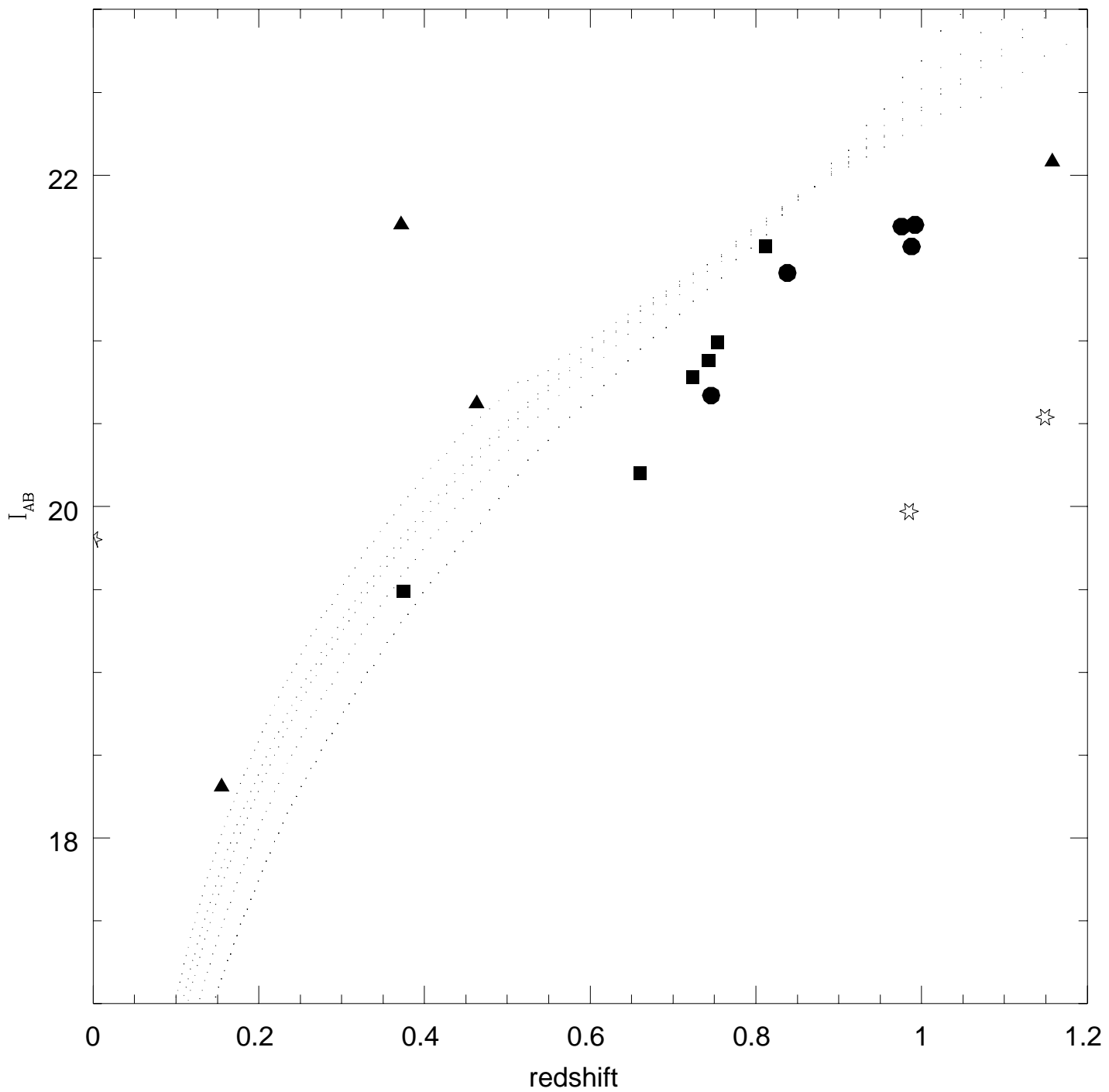
REFERENCES

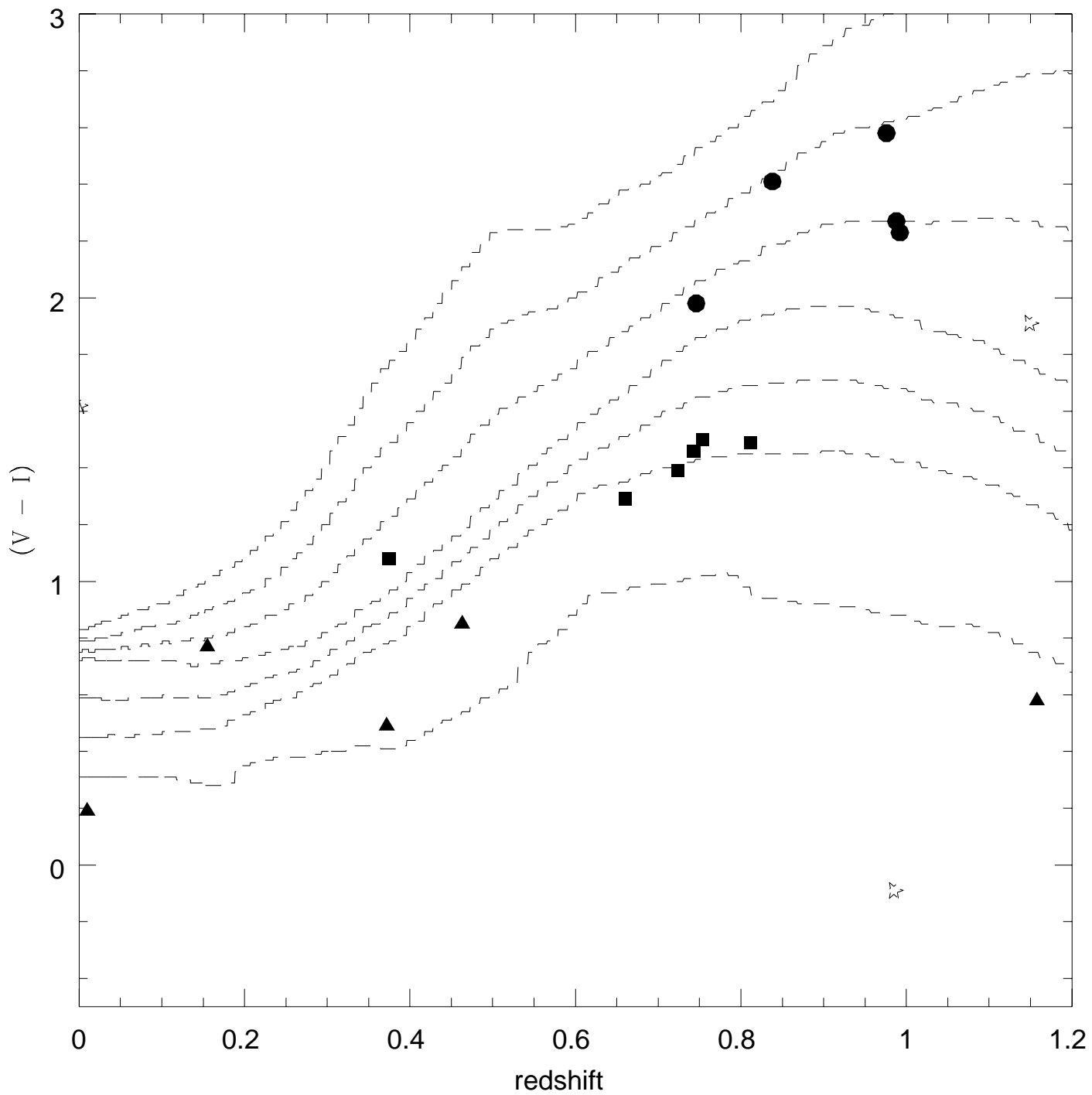
- Benn, C.R., Rowan-Robinson, M., McMahon, R.G., Broadhurst, T.J., Lawrence, A., 1993, MNRAS, 263, 98
 Bruzual, G., Charlot, S., 1993, ApJ, 405, 538
 Colless, M., Ellis, R., Taylor, K., Hook, R., 1990, MNRAS, 244, 408
 Condon, J.J., 1989, ApJ, 338, 13
 Condon, J.J., 1992, A&A Review, 30, 575
 Condon, J.J., Mitchell, K.J., 1984, AJ, 89, 610
 Dressler, A. & Gunn, J., 1983, ApJ, 270, 7
 Downes, A., Peacock, J., Savage, A., Carrie, D., 1986, MNRAS, 218, 31
 Dunlop, J., Peacock, J., Savage, A., Lilly, S., Heasley, J., Simon, A., 1989, MNRAS, 238, 1171
 Fomalont, E.B., Windhorst, R.A., Kristian, J.A., Kellerman, K.I., 1991, AJ, 102, 1258 (FWKK)
 Le Fèvre, O., Crampton, D., Hammer, F., Lilly, S., Tresse, L., 1994, ApJ, 423, L89
 Le Fèvre, O., Crampton, D., Lilly, S., Hammer, F., Tresse, L., 1995, in preparation, (CFRS II)
 Lilly, S., Hammer, F., Le Fèvre, O., Crampton, D., 1995, in preparation (CFRS III)
 Lilly, S., Le Fèvre, O., Crampton, D., Hammer, F., Tresse, L., 1995, in preparation (CFRS I)
 Oort, M., Windhorst, R., 1985, A&A, 145, 405
 Rees, M., 1984, ARA&A, 22, 471
 Rowan-Robinson, M., Benn, C.R., Lawrence, A., McMahon, R., Broadhurst, T., 1993, MNRAS, 263, 123
 Thuan, T.X., Condon, J.J., 1987, ApJ, 322, L9
 Tresse, L., Hammer, F., Le Fèvre, O., Proust, D., 1993, A&A, 277, 53
 Tresse, L., Rola, C., Hammer, F., Stasinska, G., Crampton, D., Le Fèvre, O., Lilly, S., 1994, in preparation
 Veilleux, S., Osterbrook, D.E., 1987, ApJ S., 63, 295
 Wall, J., Benn, C., Grueff, G., Vigotti, M., 1986, in Highlights Astr., Vol. 7, ed. J.P. Swings (Dordrecht:Reidel), 345.
 Wall, J., Shimmins, A., Merkelijn, K., 1971, Aust. J. Phys. Astrophys. Suppl., 19, 1
 Windhorst, R.A., 1984, PhD thesis, Univ. Leiden
 Windhorst, R.A., Dressler, A., Koo, D., 1987, in Hewitt, A., Burbidge, G., Fang L.Z., eds, Proc. IAU Symp. 124, Observational Cosmology, Reidel, Dordrecht, p. 573
 Windhorst, R.A., Fomalont, E., Partridge, R., Lowenthal, J., 1993, ApJ, 405, 498
 Wrobel, J.M., Heeschen, D., 1984, ApJ, 335, 677
 Wrobel, J.M., Heeschen, D., 1991, AJ, 101, 148

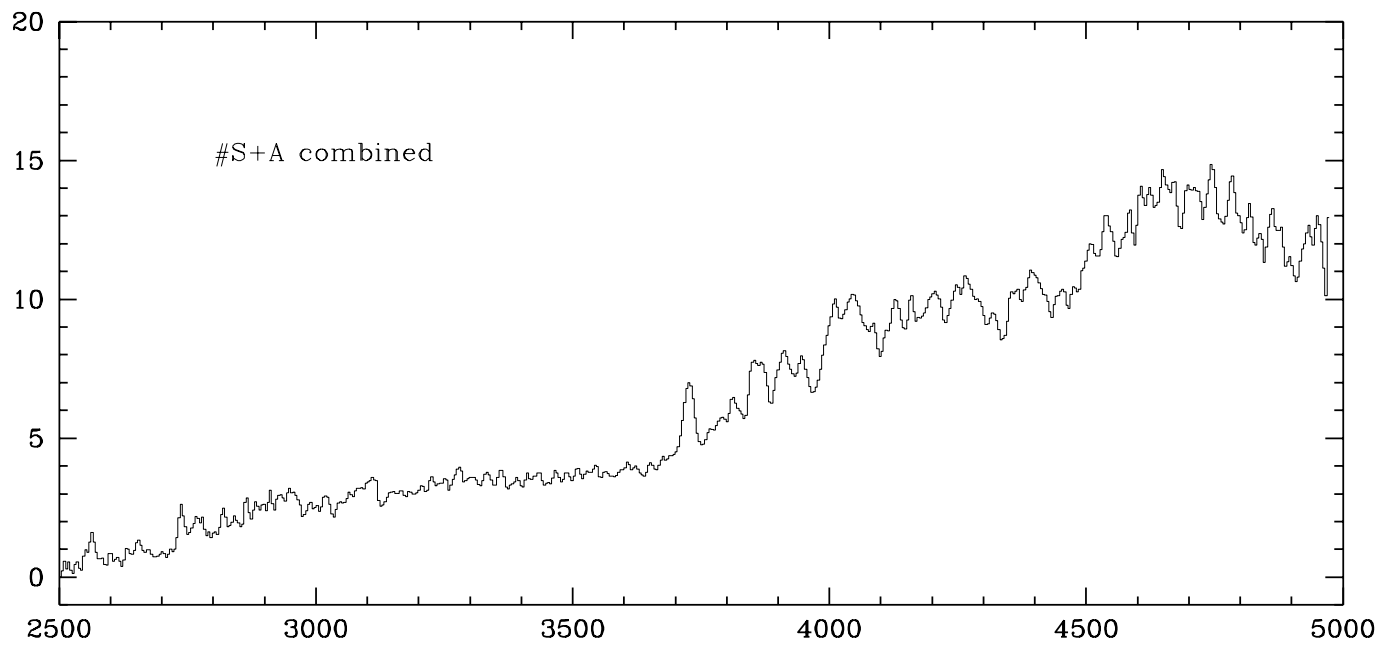
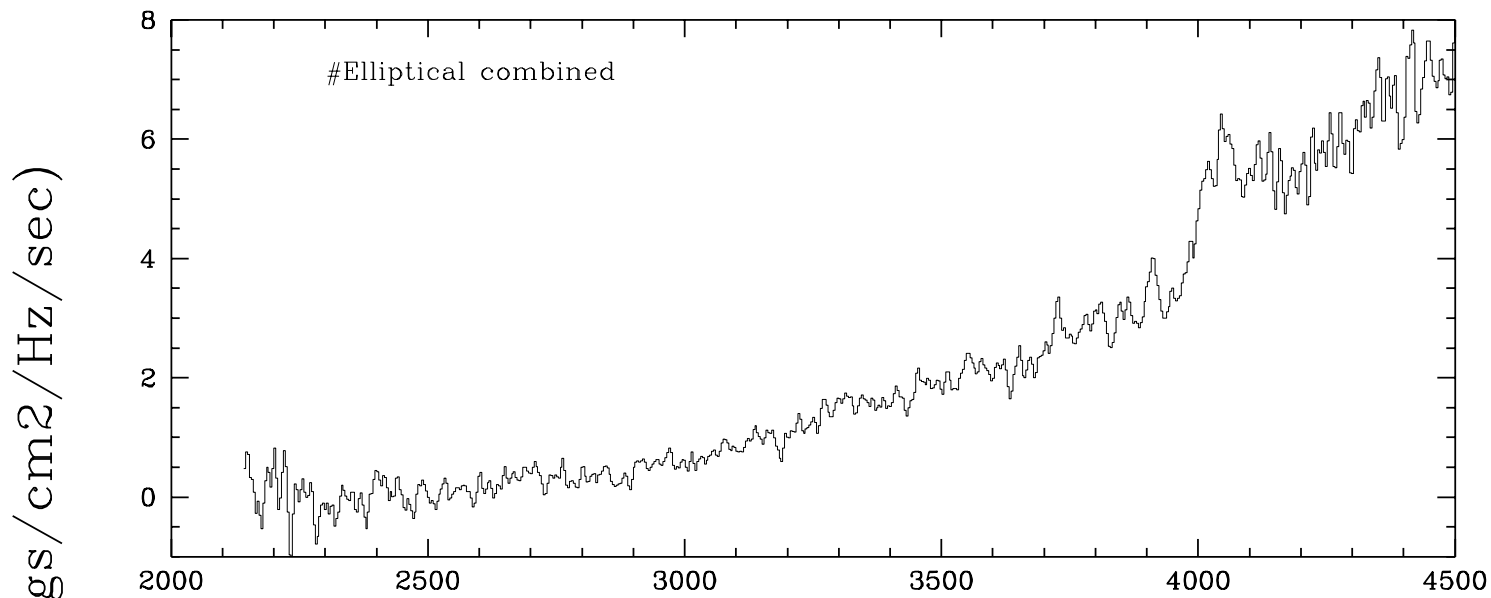












(Angstroms)

